FIELD CONSOLIDATION OF VARVED CLAY

Report No. 5
(Laboratory Shear Strength)

by
Richard P. Long, Associate Professor
Kent A. Healy, Associate Professor

JHR 75-89 Project 70-3
June, 1975

This research was sponsored by the Joint Highway Research Advisory Council of the University of Connecticut and the Connecticut Department of Transportation, and was carried out in the Civil Engineering Department of the University of Connecticut.

FIELD CONSOLIDATION OF VARVED CLAY

REPORT NO. 5

TABLE OF CONTENTS

INTRODUCTION

The research proposal, "A Study of the Field Consolidation of Varved Clay", approved by the JHRAC in 1970 included a laboratory investigation of shear strength. This report describes the laboratory investigation and results to date.

BACKGROUND

The alternate layering of the silt and clay varves and the stresses due to gravity produce anisotropic consolidation and shear strength characteristics. The rates of consolidation observed in the field are higher than measured in the laboratory, probably due to drainage through the silt varves. (1)* (2) (3) Unconsolidated undrained triaxial shear tests performed on samples trimmed from blocks of varved clay showed lower shear strengths when the varves were oriented at 45 and 60° angle to the axis of the samples, than when oriented at 90° or 0° to the axis, indicating lower shear strength along the varves than across them.

The consolidation of the varved clay that occurs during the construction of an embankment on it increases the strength of the soil. Therefore, unconsolidated-undrained tests on samples taken prior to construction underestimate the available soil strength at the end of construction even if perfect soil samples are used in the test.

To accurately predict the field behavior of soil, it is necessary to subject undisturbed samples of the soil in the lab to the same stresses, in the same sequences, as are anticipated in the field. Field sampling relieves the original stresses in the soil samples that are eventually tested in the

*Numbers in parentheses indicate references at the end of the text.

laboratory. This obstacle is normally overcome by reconsolidating the sample to the original stress system before any additional stresses are applied. In the case of varved clay, this would mean applying a K_o stress system, keeping the major principal stress perpendicular to the varves and the minor principal stress parallel to the varves. Hopefully, this brings the sample back to the condition existing in the soil before any embankment stresses are applied.

Another difficulty is applying the stresses to the sample that will occur due to the weight of the embankment. States of stress induced by embankment construction orient the major principal stresses in the foundation soil as shown in Fig. 1. In the vicinity of "A", the major principal stress is in the vertical direction perpendicular to the varves. The major principal stresses from the embankment load will be horizontal along the varves in the vicinity of "C". At an intermediate point such as "B", the major principal stresses will be oriented at 45° to the varves. During the construction process, the imposed stresses will cause additional consolidation. The in situ and applied stress at "A" are illustrated in Fig. 2. The subscript "a" indicates stresses due to embankment load.

The stresses on sample "C" at some distance from the center line of the embankment are as shown in Fig. 3. The subscripts "a" again refer to applied stresses. The principal stresses due to the embankment are rotated 90° to the in situ principal stresses. It should be noted that for samples A and C shearing takes place across the varves, not revealing any differences in strength that might occur along the varves as in the vicinity of point "B". The sequence of stress systems that would have to be applied to sample B in order to show the weakness along the varves would be as shown in Fig. 4.

In addition to the problem of principal stress rotation, most field situations are plane strain conditions.

1. First reconsolidate the clay under K_o condition to overcome sampling disturbance.
2. Then rotate the principal stress by 30 or 45° to simulate the shearing stresses that are applied during embankment construction.

The only shear apparatus that approaches these conditions is the Direct Simple Shear Device, but the principal stresses continue to rotate throughout the test.

What has normally been done is reconsolidation of the samples as shown in Fig. 5, either isotropically or anisotropically and then increase σ_1, while holding σ_3 constant, to cause shear failure. This sequence of stressing does cause shearing along the varves but does not simulate the K_o consolidation that has preceded the shearing phase, and the relation of the strength to the field situation is unclear.

This report describes a series of unconsolidated-undrained triaxial shear tests run on samples with the varves at angles of 0, 30, 45, 60 and 90° to the axis of the sample and a series of isotropically consolidated-undrained triaxial shear tests on samples with the varves at angles of 0, 45 and 90° to the axis. In some of these latter tests, the pore pressure was measured during the shearing.

Strength Parameters

The triaxial tests measured the following parameters:

1. S_u - undrained strength
2. $\bar{\phi}$ - effective friction angle
3. $\bar{c}$ - effective cohesion

It was assumed that the Mohr-Coulomb failure criterion applied to the varved clays. On the basis of effective stresses, the strength on the failure plane at failure is given by the equation:

$$T_{ff} = \bar{c} + \bar{\sigma}_{ff} \tan \bar{\phi} \qquad (1)$$

where T_{ff} = shear stress on the failure plane at failure and

$\bar{\sigma}_{ff}$ = normal effective stress on the failure plane at failure.

$\bar{c}$ and $\bar{\phi}$ as defined before.

The undrained strength S_u was measured on the basis of total stresses acting on the sample at failure, and assuming $\phi = 0$.

$$S_u = \frac{\sigma_{1f} - \sigma_{3f}}{2} \qquad (2)$$

where: σ_{1f} and σ_{3f} are the major and minor principal total stresses acting on the sample at failure. Failure was taken as the maximum shear stress that the sample could resist.

To facilitate data analysis, q, p, $\bar{p}$ plots were used instead of Mohr's Circles. Use of these plots allows an entire Mohr's Circle to be represented by a single point and facilitates the location of failure envelopes. The values can be defined in terms of principal stresses in the triaxial test with the equations:

$$q = \frac{\sigma_v - \sigma_h}{2} = \frac{\bar{\sigma}_v - \bar{\sigma}_h}{2}$$

$$p = \frac{\sigma_v + \sigma_h}{2}$$

$$\bar{p} = \frac{\bar{\sigma}_v + \bar{\sigma}_h}{2} \qquad (3)$$

where $\bar{\sigma}_v$, σ_v = respectively the effective and the total principal stress in the vertical direction and $\bar{\sigma}_h$, σ_h = respectively the effective and total principal stresses in the horizontal direction.

The failure envelope is defined by:

$$q_f = \bar{a} + \bar{p}_f \tan \bar{\alpha} \qquad (4)$$

where: α = the angle between the failure line and the $\bar{p}$ axis. a = intercept on the vertical axis. The subscript "f" denotes the values at failure.

The effective friction angle can readily be computed from this plot by the relation:

$$\sin \bar{\phi} = \tan \bar{\alpha} \qquad (5)$$

Samples Used in the Tests

Blocks of varved clay (2' x 2' x 1') were obtained from near the surface of a clay pit owned by the Kelsey-Ferguson Brick Co. in East Windsor, Ct. and stored in a room having high humidity. Samples for testing were cut from the blocks and trimmed to a diameter of 1.4 inches and a height of 3.0 inches.

In some blocks both the silt and clays had a grey color; in others they appeared brown. Preliminary tests showed that the difference in color correlated with a difference in some strength properties, the grey clay being the weaker of the two in unconsolidated-undrained strength. This difference became less pronounced in tests involving reconsolidation.

The brown clay showed distinct anisotropic behavior in the unconsolidated-undrained test and approximately the same drained strength parameters as the grey. The majority of the tests were therefore made with the brown clay. There was, however, some variation in strength properties among samples of the brown varved clay. These variations among brown clay samples correlated with differences in the initial water contents. The greater the initial water content, the lower the strength. The initial series of tests were compression tests (σ_1 always vertical).

For the investigation of anisotropic strength properties, the samples were trimmed so that the varves formed a predetermined angle θ with the horizontal. In this way, the effect of the relative orientation of the varves and principal stresses could be studied.

Compression Testing

The samples were placed into a rubber membrane and secured to the pedestal with rubber "o" rings, under water to eliminate air bubbles between the soil and the membrane. The tests were made in a Wykeham Farrance triaxial test machine. This apparatus is a constant-rate-of-strain device. The following types of test were run:

1. Unconsolidated-Undrained (UU) (with and without pore pressure measurements)
2. Consolidated-Drained (CD)
3. Consolidated-Undrained (CU) (with and without pore pressure measurements)

All of the tests were run so that the vertical stress on the specimen was the major principal stress. Only isotropic consolidation was used.

For the consolidated-drained tests and the consolidated-undrained tests with pore pressure measurements, the times to failure were computed beforehand and the approximate strain rate set on the triaxial apparatus. The methods of computing times to failure are shown in the Appendix.

Results

1. Unconsolidated-Undrained Tests (UU)

UU tests were run on two series of samples. The strengths correlated with the natural water content of the recovered samples here referred to as

the initial water contents. One series had an initial water content of approximately 50%. The second series had an initial water content of approximately 60%.

Each series investigated the effect of the orientation of the major principal stress to the direction of the varves on undrained strength. The results of these sets of tests are shown in Fig. 6 and 7.

In Fig. 6, the undrained strength S_u for Brown Varved clay at W_o = 50% is plotted against the angle (θ) that the varves made with the horizontal during the test. The direction of the major principal stress was always vertical. Fig. 7 shows the same information for the Brown Varved Clay at W_o = 60%. As can be seen from Fig. 6 and 7 the undrained strength decreased as the angle between the direction of the varves and the major principal stress approached 45° from either direction. Considering each water content separately, the S_u's were about the same when the major principal stress was both perpendicular and parallel to the varves. For this first series of S_u's at an initial water content W_o = 50% the orientation of the varves was 0, 30, 45, 60 and 90° to the horizontal. Subsequent tests studied the effects at 0, 45 and 90, since the variation of strength was greatest among these three. The variation in strength with direction appears to be more pronounced for the series having an initial water content W_o = 50%. The S_u's for the samples having a W_o = 60% were always smaller.

Fig. 8 compares the S_u with orientation of varves for UU tests and CU tests. The consolidation in these tests was isotropic. The UU tests were run with chamber pressures of 20 and 60 psi, but no consolidation was allowed. In the CU tests, the samples were first allowed to consolidate isotropically under the chamber pressure, then failed undrained. The consolidating chamber pressures were 20 and 60 psi. Comparing the data in Fig. 8 shows that the orientation of varves is diminished by isotropic consolidation. The gain in

strength due to consolidation is greater for the 45 degree orientation of the varves than it is for either the zero or 90° orientation. Consolidation to 20 psi shows this relative increase which continues up to 60 psi.

2. Consolidated Undrained Tests

Consolidated undrained tests yield information on the increase of strength with increase in effective stress. With pore pressure measurements during the undrained shear, the effective stress envelope and the undrained strength diagram can be determined by one series of tests. However, in this series of tests, the lack of consolidation similar to the field must be noted. CU tests with pore pressure were run with the varves oriented at 0°, 45° and 90° to the horizontal. Times to failure were again computed prior to testing to insure that a proper value of pore pressure was being detected during the end of the test. The results from these tests are plotted in Figs. 9, 10 and 11. Fig. 9 shows the drained and undrained behavior with the varves at 0° to the horizontal. The dashed lines indicate the effective stress paths. Figs. 10 and 11 show similar information with the varves at 45° and 90° respectively.

The effective stress envelopes at the higher stress levels extrapolate through the origin. The undrained plots indicate a break due to a maximum past pressure somewhere before the first consolidation pressure. Both these plots indicate a possible change in structure caused by the isotropic consolidation. The slope of the undrained envelope is about half the slope of the drained envelope. The measured A_f for samples consolidated to 20 psi is about 0.5. At consolidating pressures of 40 psi and above, A_f approached 1.0. A summary of the data obtained from these tests is shown in Table I of the appendix.

Consolidated undrained tests were also run on a series of samples having W_o = 61%. These results are shown in Fig. 12. The slope of the curve is

flatter than the samples with a lower initial water content, and the extrapolated curve does not pass through the origin.

3. Consolidated Drained Tests

A series of samples were tested in a consolidated drained state. The initial water content for these samples was approximately W_o = 61%. The samples were first consolidated to a selected chamber pressure (10, 20, 30 and 40 psi) then sheared drained along one of the stress paths shown in Fig. 13. The time to failure for the shearing portion of the test was computed based on the coefficient of consolidation observed as the water was expelled from the sample under the isotropic chamber pressure. The test times varied between 2 and 47 hours depending on the sample and the level of stress. As can be seen from Fig. 13, no significant intercept on the vertical axis was observed.

The relations among the water contents and the stress parameters $\bar{p}_o$, $\bar{p}_f$ and q_f are shown for the tests involving consolidation in Figures 14 and 15. The plots of these parameters as straight lines on semilog paper indicate normally consolidated behavior. Previous one-dimensional consolidation indicated that varved clay in this area is overconsolidated. The behavior indicated in Figures 14 and 15 may be due to isotropic consolidation.

Extension Testing

Unconsolidated - Undrained extension tests were run on varved clay samples. To accomplish this type test, which is an unloading, a double ball and socket connection was used between the loading ram and the proving ring as shown in Fig. 16. The sample in Fig. 16 is set up for pore pressure measurements. However, difficulty was experienced with the electronic equipment and all the tests were run without pore pressure measurements.

Two differences in behavior were observed between the extension tests and the compression tests. Most of the samples in the compression tests formed a visible failure surface that was a plane at approximately $45° \pm$ with the principal stresses. The failure modes for the samples in the extension test usually involved a reduction in sample cross-sectional area. Some typical failure shapes of samples in the extension tests are shown in Fig. 17.

The second distinction between samples failed in compression and samples failed in extension is the large strains required to cause failure in extension. Failure in an extension test required about 20 to 25% strain to reach a peak stress value. Failure in undrained compression tests on the other hand required only 5 to 10% strain to reach peak stress.

The results of the extension tests are shown in Fig. 18. The effect of anisotropy, while evident in Fig. 18, is more difficult to interpret and will require more study.

Conclusions

1. The unconsolidated-undrained strength behavior of the varved clay in the overconsolidated state is anisotropic and depends on the orientation of the major principal stress to the varves.
2. Equipment limitations at the present time make it impossible to properly test for these anisotropic properties in the consolidated-undrained test.
3. The variation of strength along a failure surface can be substantial; therefore, further research is required to optimize foundation design for fills and structures on this soil.

References

1. Long, R.P. and K.A. Healy, "Preliminary Report, Field Consolidation of Varved Clay Phase I. Department of Civil Engineering, University of Connecticut, JHR-PR 71-34, 1971

2. Long, R.P. and K.A. Healy, Field Consolidation of Varved Clay, Report No. 2 Department of Civil Engineering, University of Connecticut, JHR 71-38, 1971

3. Long, R.P. and K.A. Healy, Field Consolidation of Varved Clay Report No. 3, Civil Engineering Department, University of Connecticut, JHR 72-55, 1972

Table I

Summary of Data on CU Tests with

Pore Pressure Measurements w_o = 53-55%

θ	σ_c psi	S_u (psi)	A_f	Δu	σ_{3f}	σ_{1f}	$\bar{\sigma}_{1f}$	$\bar{\sigma}_{3f}$	$\frac{\bar{\sigma}_{1f} - \bar{\sigma}_{3f}}{\bar{\sigma}_{1f} + \bar{\sigma}_{3f}}$
0°	20 psi (No. 79)	9.0	+0.5	+9.35	20 psi	38	28.65	10.65	0.46
	40 psi (No. 71)	12.4	+1.1	+27.2	40 psi	64.8	37.6	12.8	0.49
	60 psi (No. 73)	17.0	+1.1	+37	60 psi	94	57	23	0.425
90°	20 psi (No. 72)	9.0	+0.5	+9	20 psi	38	29	11	0.45
	40 psi (No. 70)	13.0	+1.0	+25.4	40 psi	66	40.6	14.6	0.47
	60 psi (No. 69)	22.5	+1.0	+34.4	60 psi	105	70.6	25.6	0.47
45°	20 psi (No. 80)	9.0	0.5	9	20 psi	38	29	11	0.45
	40 psi (No. 81)	9.5	1.2	23.2	40 psi	59	35.8	16.8	0.36
	60 psi	15.0	1.2	34.5	60 psi	90	55.5	25.5	0.37

LEGEND FOR FIGURES

Fig. 1 Orientation of Principal Stresses Along Failure Surface

Fig. 2 Stresses at A

Fig. 3 Stresses at C

Fig. 4 Stresses at B

Fig. 5 Stresses in Lab Tests

Fig. 6 Variation of S_u with Orientation of Varves for Brown Varved Clay $W_o = 50\%$

Fig. 7 Variation of S_u with Orientation of Varves for Brown Varved Clay $W_o = 60\%$

Fig. 8 Variation of S_u with Orientation of Varves for Consolidated Undrained Tests

Fig. 9 Consolidated Undrained Results - Varves Horizontal $W_o = 55\%$

Fig. 10 Consolidated Undrained Results - Varves at 45° to Horizontal, $W_o = 55\%$

Fig. 11 Consolidated Undrained Results - Varves Vertical, $W_o = 55\%$

Fig. 12 Consolidated Undrained Results - Varves Horizontal, $W_o = 61\%$

Fig. 13 Consolidated Drained Results - Varves Horizontal, $W_o = 61\%$

Fig. 14 Water Contents vs. Stress Plots, $W_o = 63\%$

Fig. 15 Water Contents vs. Stress Plots, $W_o = 55\%$

Fig. 16 Ram Attachment for Triaxial Extension Test

Fig. 17 Sample Failure in Extension Tests

Fig. 18 The Variation of Maximum Shear Stress in Extension Tests with Orientation of Varves and Amount of Strain

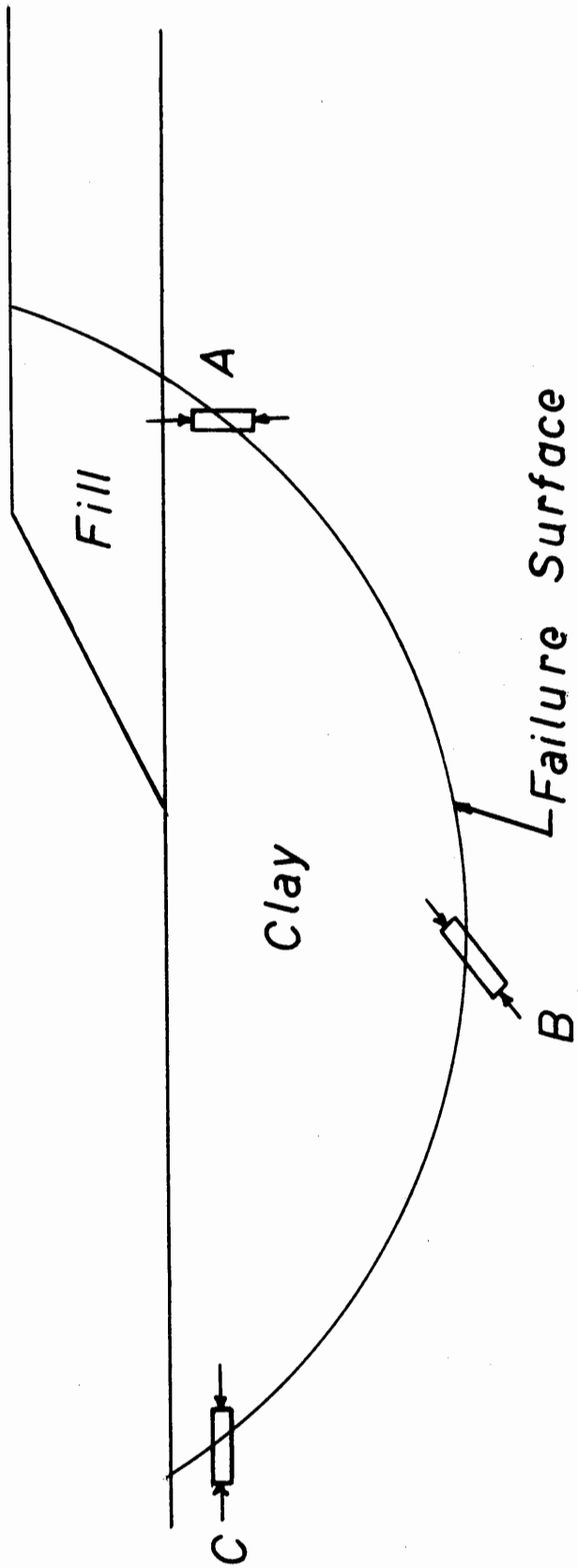

Fig 1 Orientation of Principal Stresses along Failure Surface

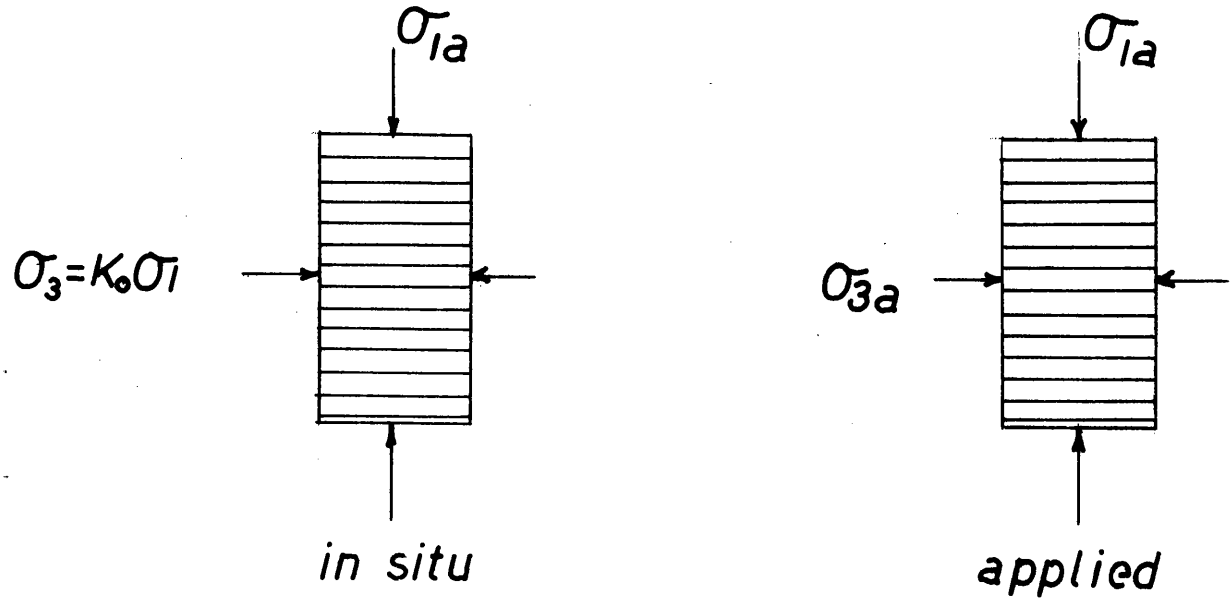

Fig 2 Stresses at A

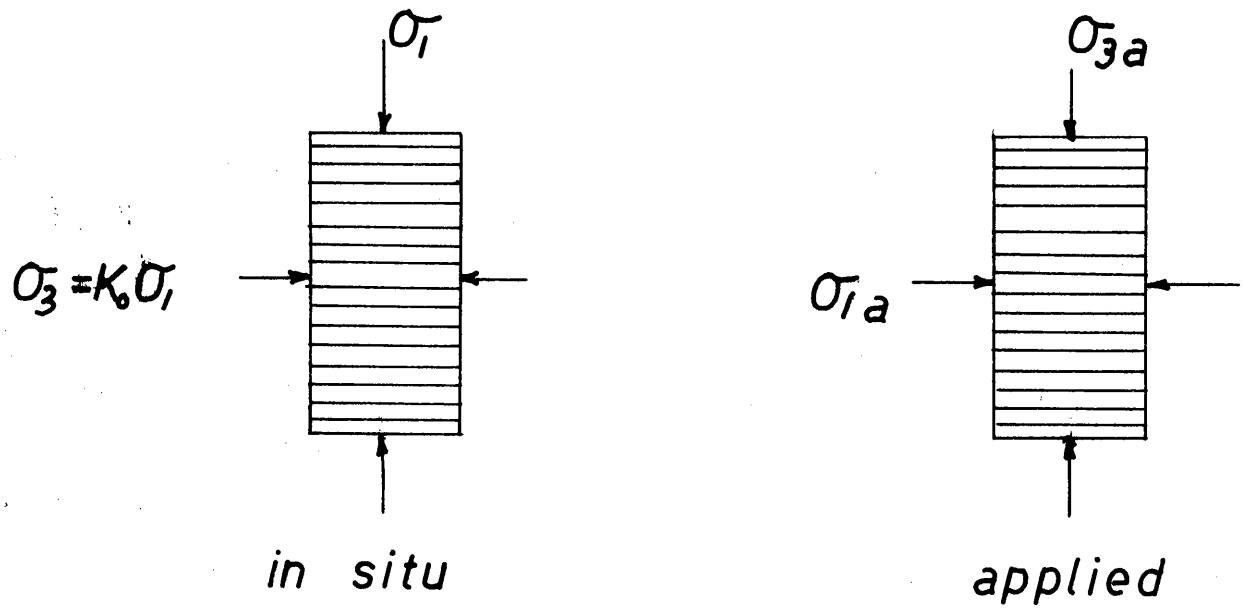

Fig 3 Stresses at C

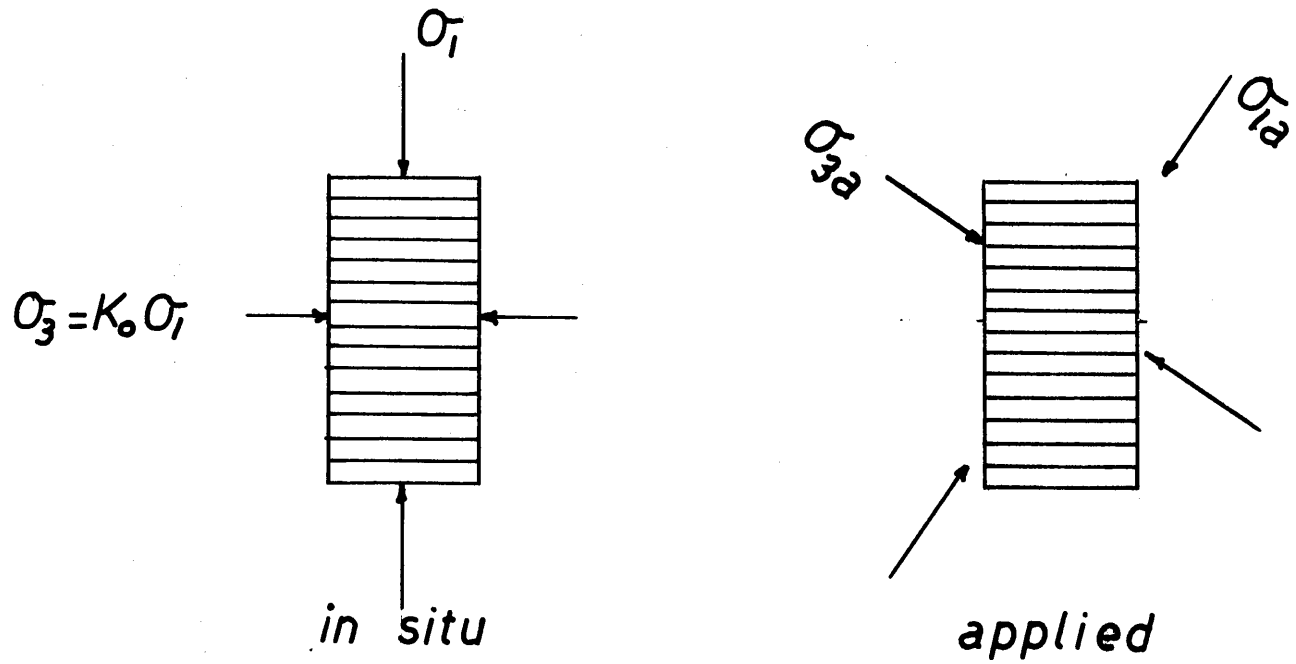

Fig 4 Stresses at B

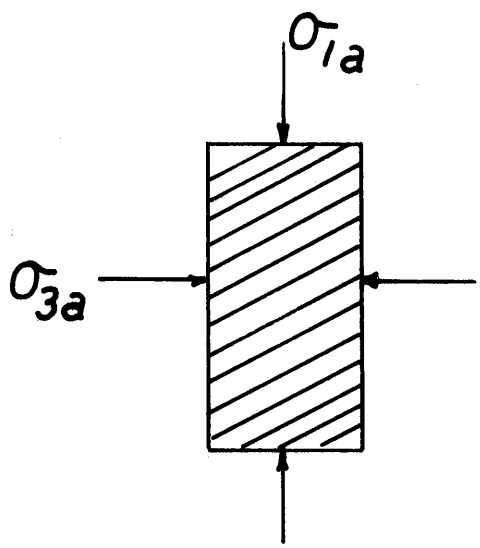

Fig 5 Stresses in Lab Tests

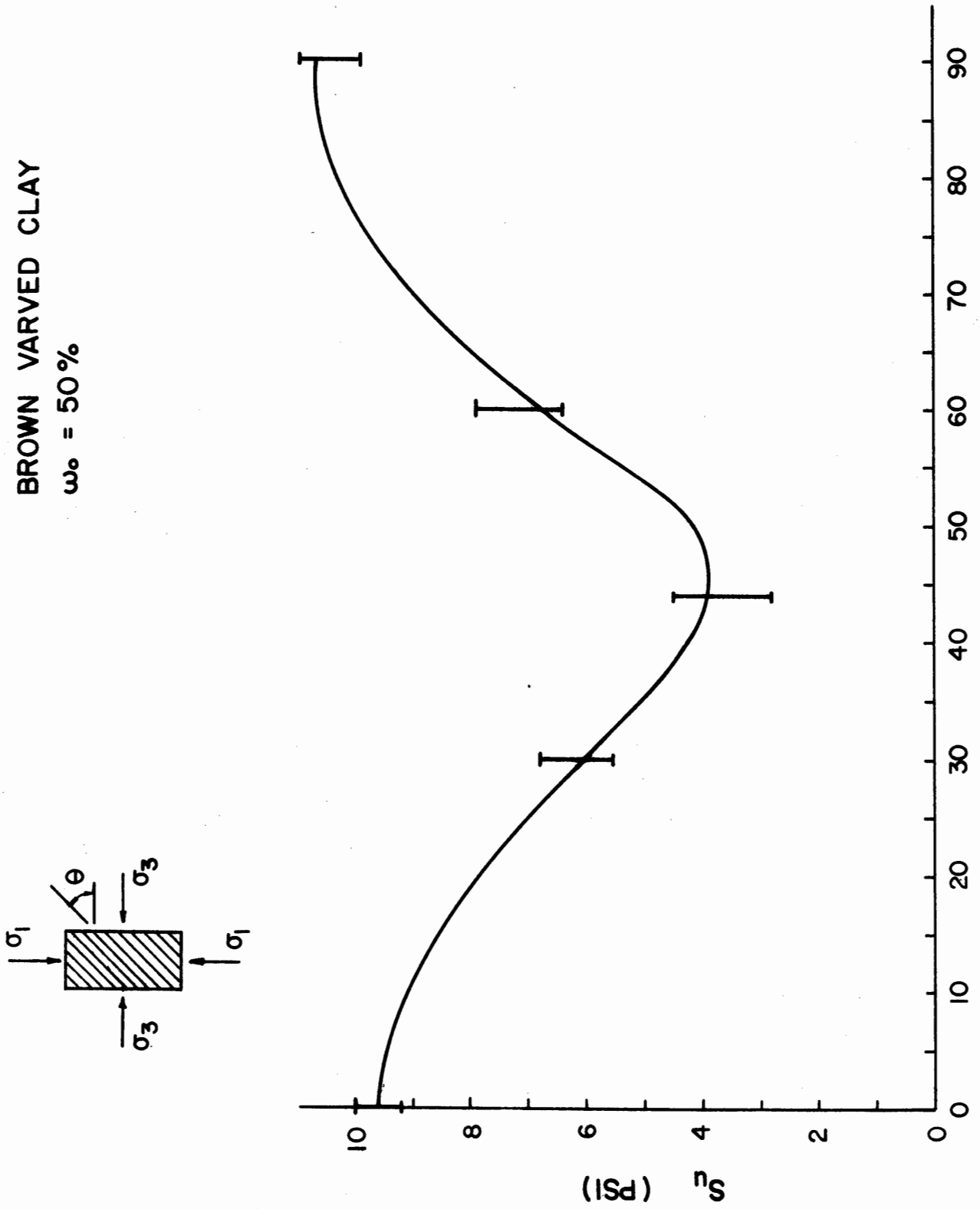
BROWN VARVED CLAY
ω₀ = 50%
σ1
σ3
θ
σ3
σ1
Su (PSI)
0
2
4
6
8
10
0
10
20
30
40
50
60
70
80
90
θ (DEGREES)

Fig 6

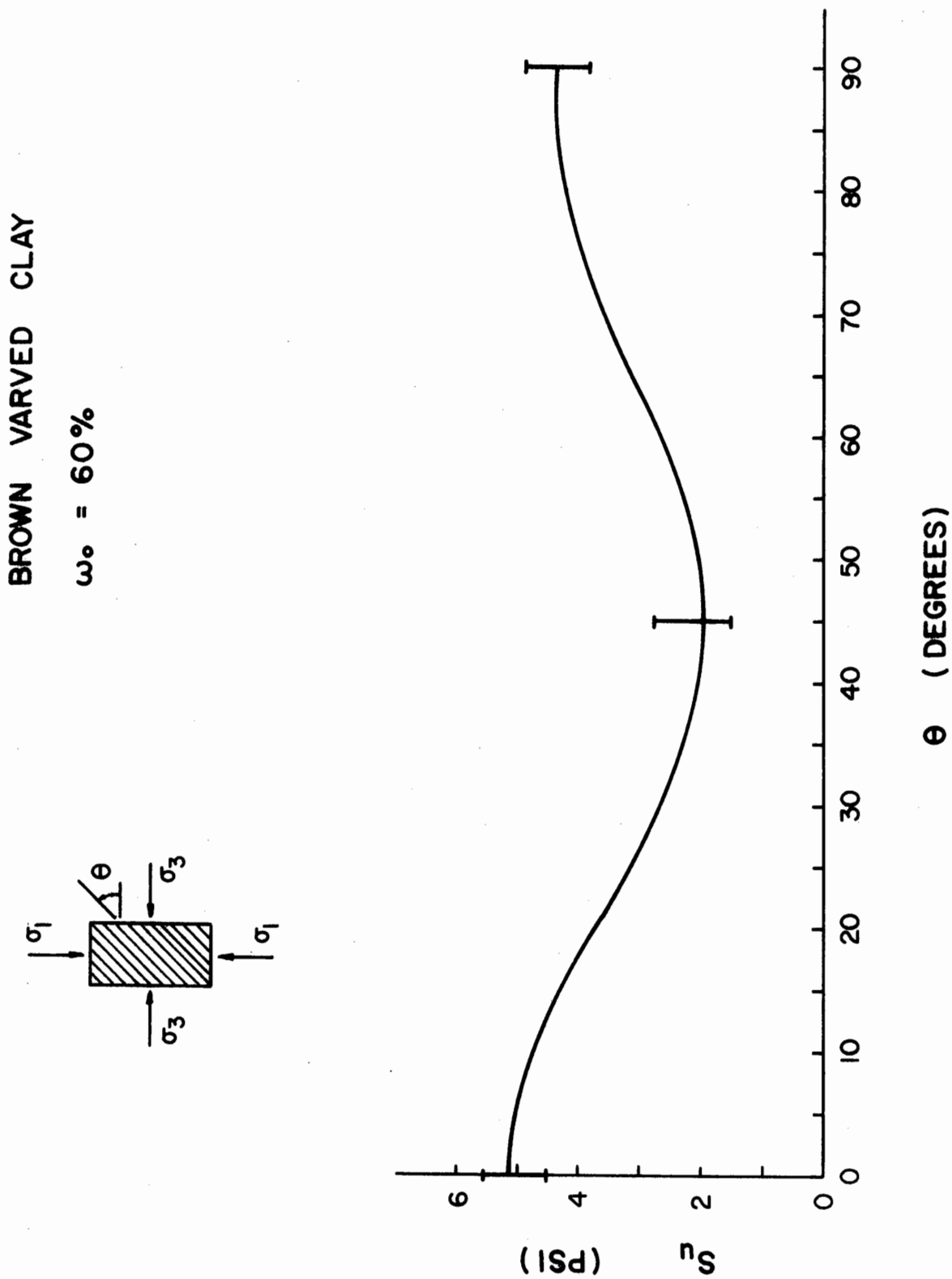
BROWN VARVED CLAY
ω₀ = 60%
σ1
σ3
θ
σ3
σ1
Su (PSI)
0
2
4
6
0
10
20
30
40
50
60
70
80
90
θ (DEGREES)

Fig 7

BROWN VARVED CLAY

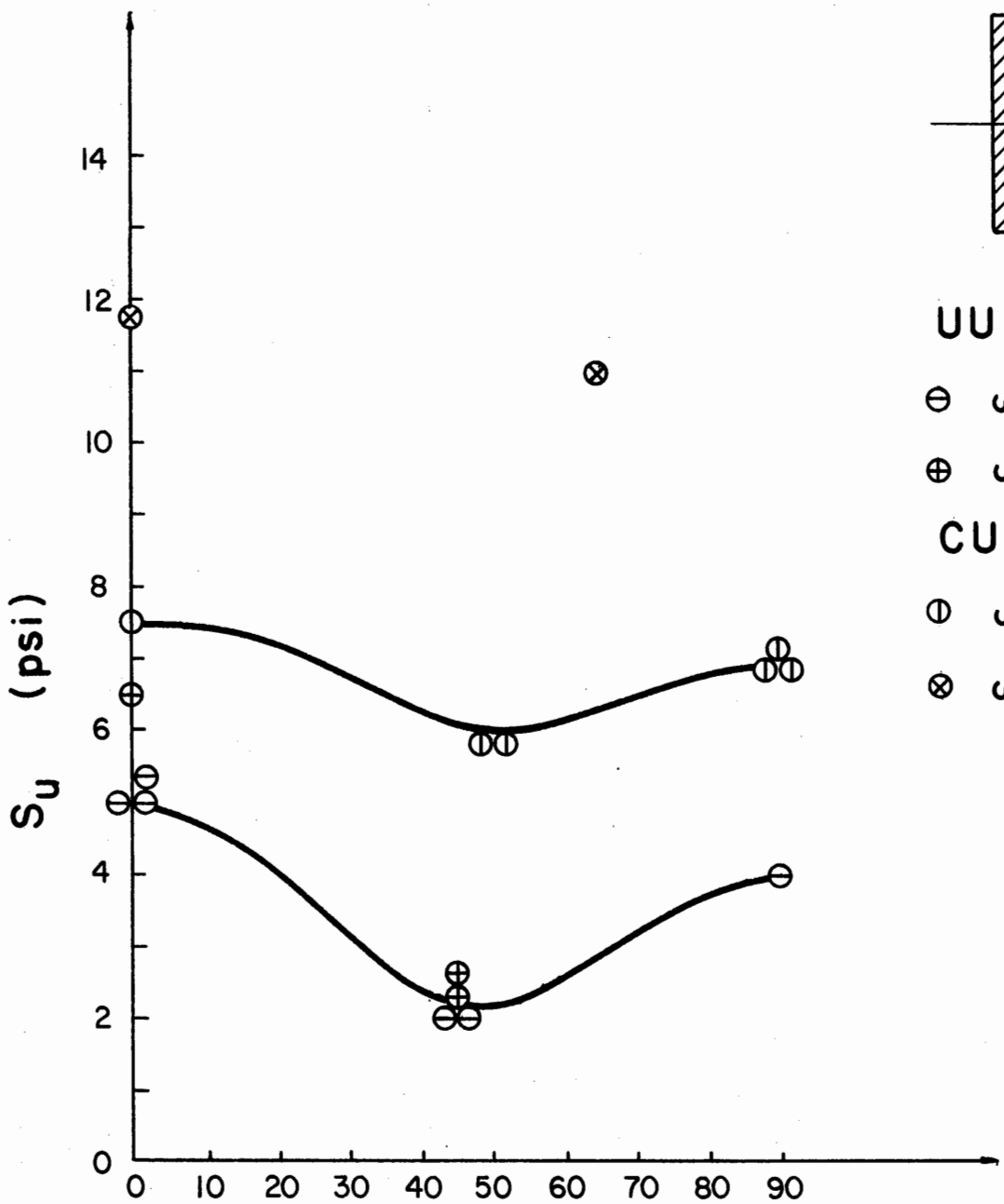

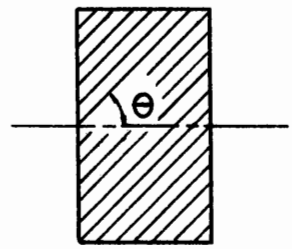

UU TEST

⊖ ω = 60%, σ_3 = 20 psi

⊕ ω = 60%, σ_3 = 60 psi

CU TEST

⊖ ω = 60%, σ_c = 20 psi

⊗ ω = 60%, σ_c = 60 psi

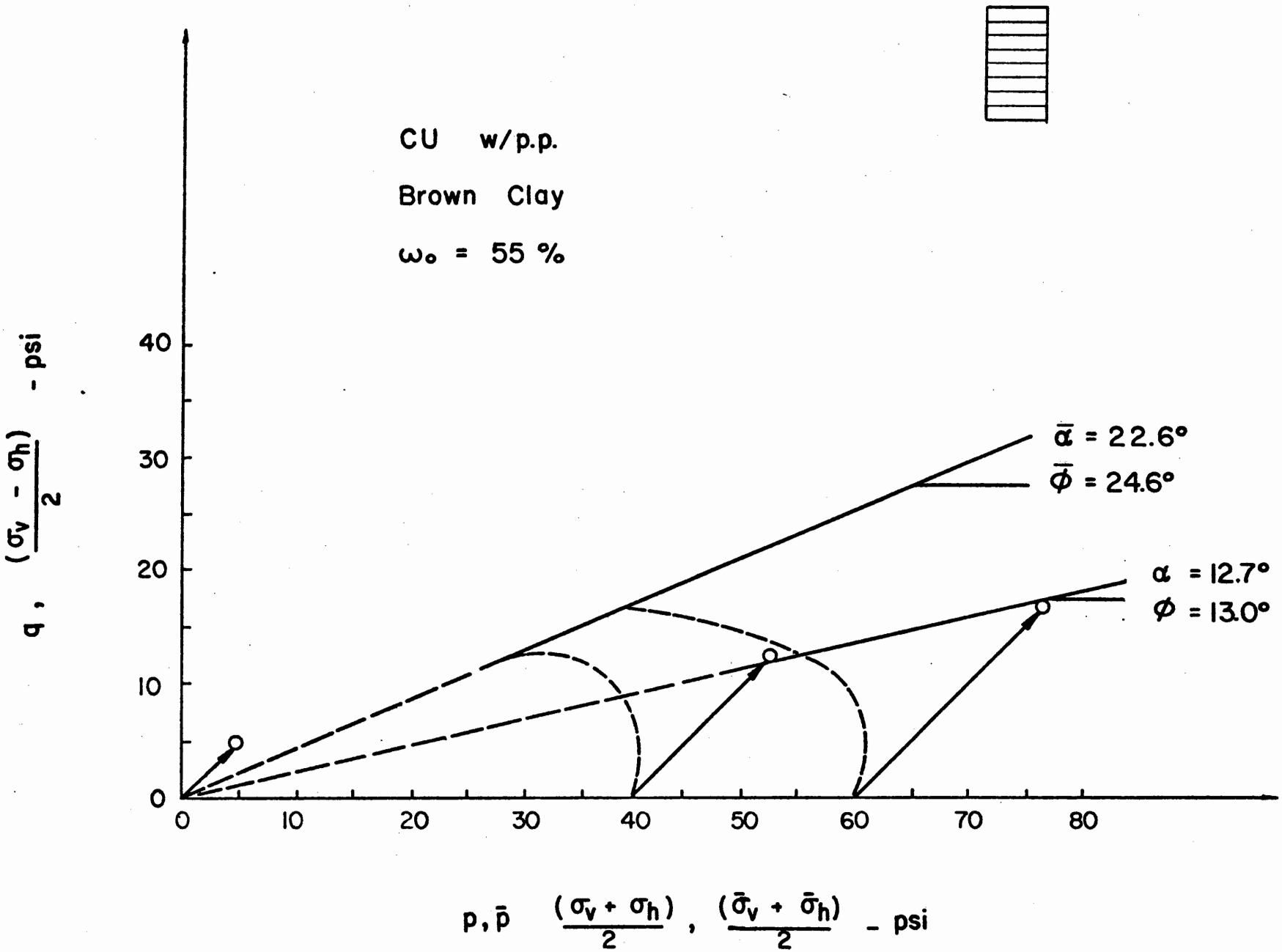
CU w/p.p.
Brown Clay
ω_o = 55 %
$\bar{\alpha}$ = 22.6°
$\bar{\phi}$ = 24.6°
α = 12.7°
ϕ = 13.0°
q , $\frac{(\sigma_v - \sigma_h)}{2}$ - psi
p, $\bar{p}$ $\frac{(\sigma_v + \sigma_h)}{2}$, $\frac{(\bar{\sigma}_v + \bar{\sigma}_h)}{2}$ - psi
0
10
20
30
40
50
60
70
80

Fig 9

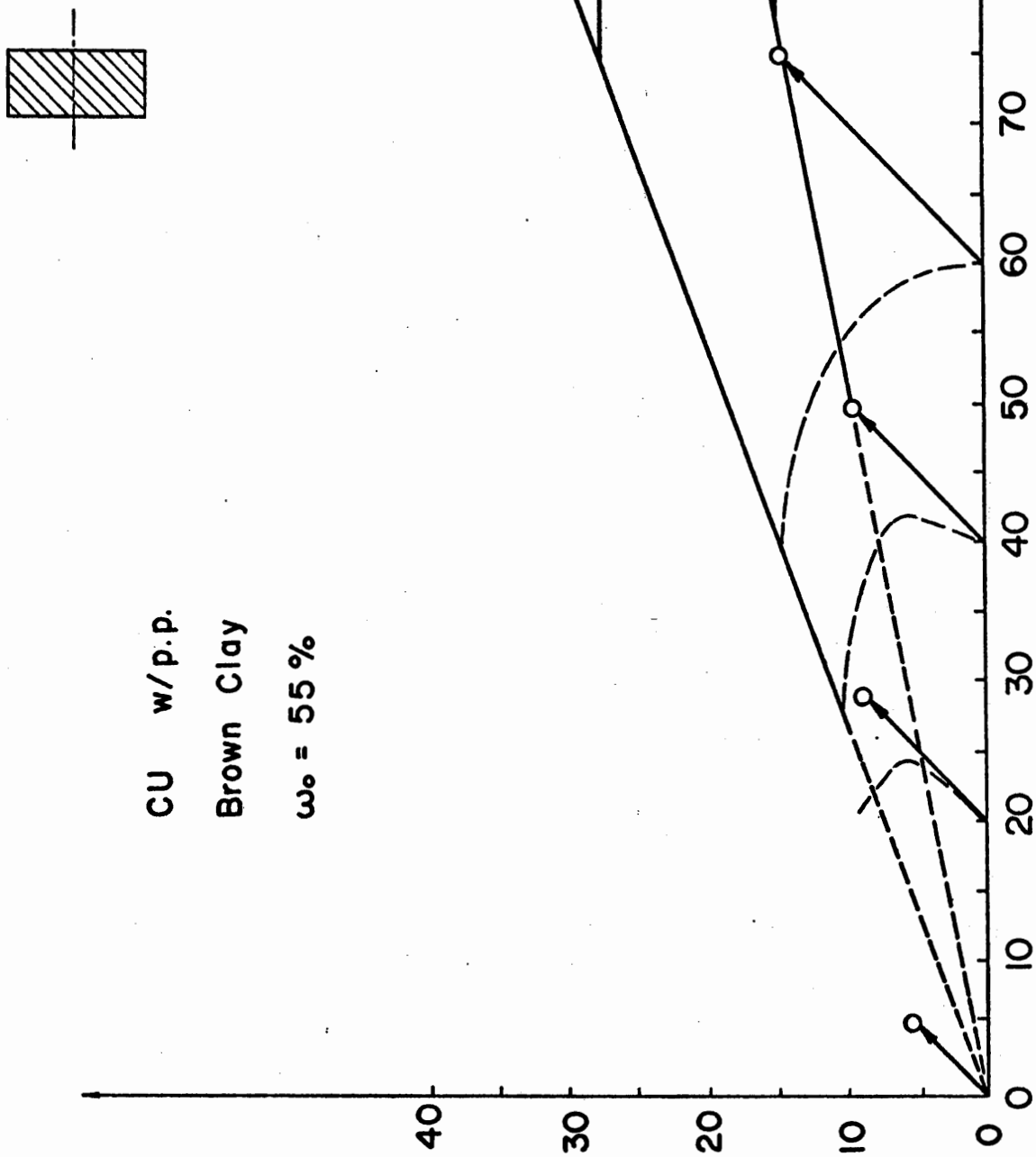
CU w/p.p.
Brown Clay
ω_o = 55 %
$\bar{\alpha}$ = 20.5°
$\bar{\phi}$ = 22°
α = 11°
ϕ = 11.1°
0
10
20
30
40
50
60
70
80
p, $\bar{p}$ ($\frac{\sigma_v + \sigma_h}{2}$, $\frac{\bar{\sigma}_v + \bar{\sigma}_h}{2}$) - psi
0
10
20
30
40
q ($\frac{q}{\sigma_v - \sigma_h}$) - psi

Fig 10

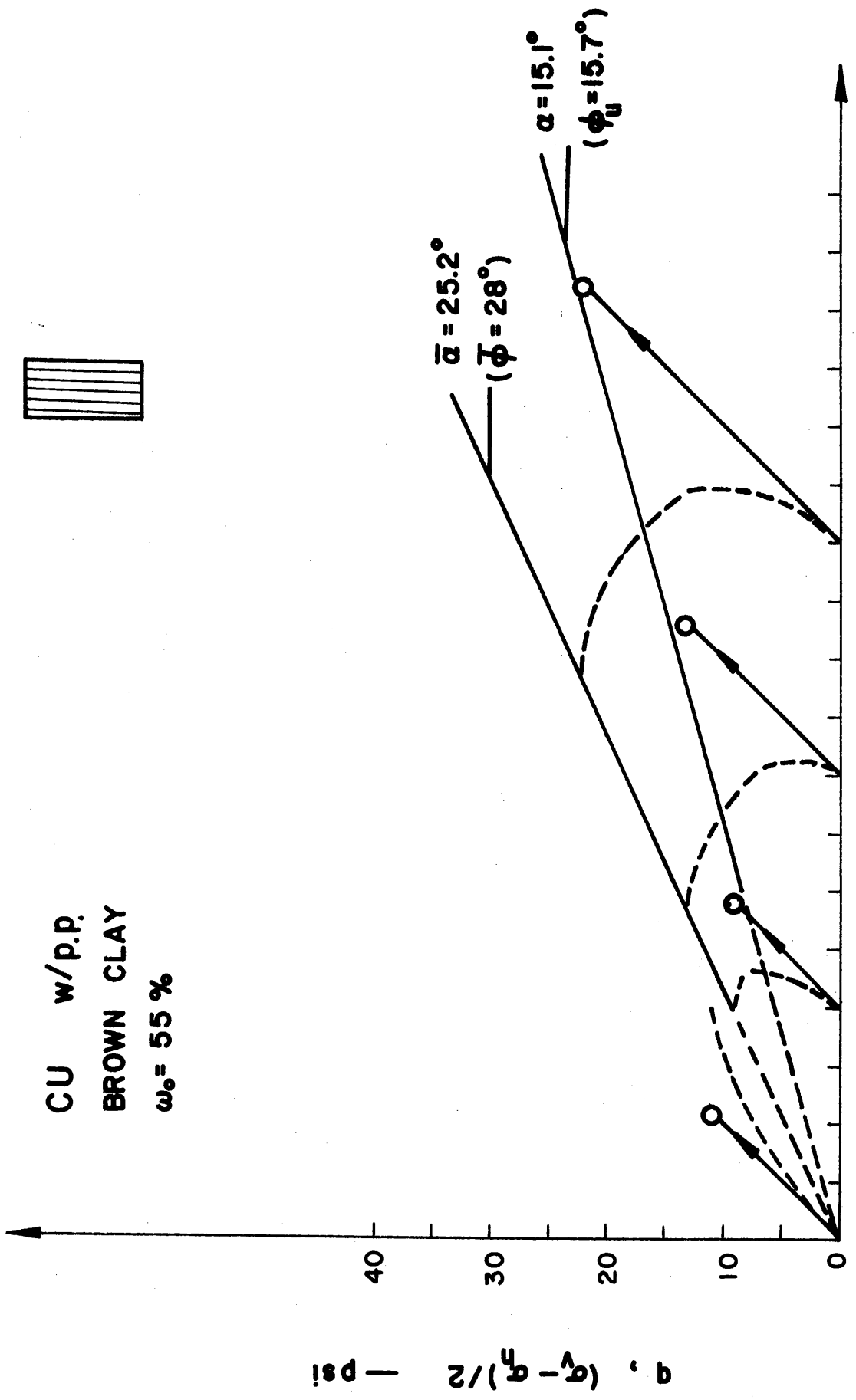
CU w/p.p.
BROWN CLAY
ω_o= 55 %
$\bar{\alpha}$ = 25.2°
($\bar{\phi}$ = 28°)
α = 15.1°
(ϕ_u = 15.7°)
q , $(\sigma_v - \sigma_h)/2$ — psi
p , $\bar{p}$ $\left(\frac{(\sigma_v+\sigma_h)}{2}, \frac{(\bar{\sigma}_v+\bar{\sigma}_h)}{2}\right)$ — psi
0
10
20
30
40
50
60
70
80
90

FIG 11

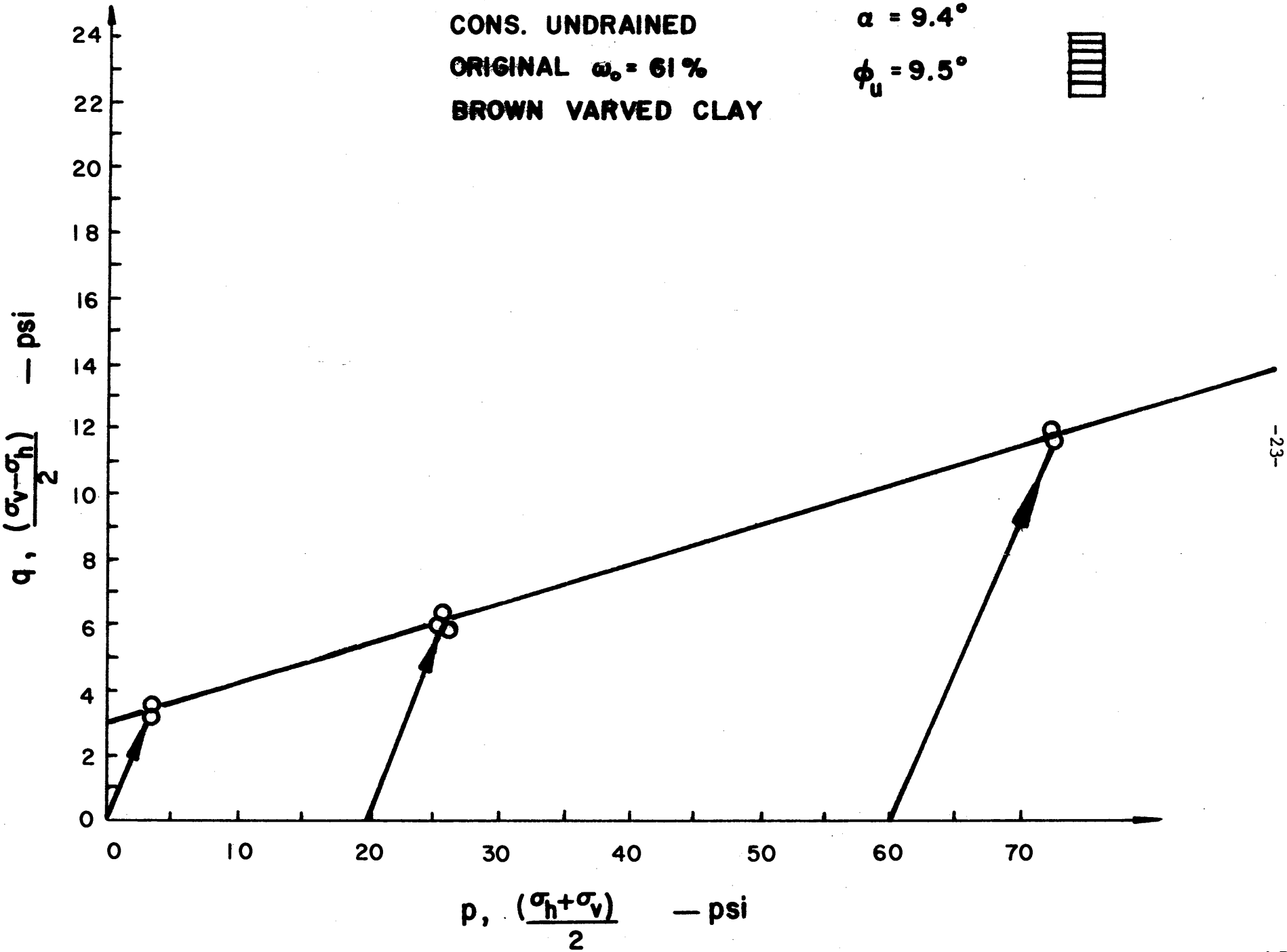
CONS. UNDRAINED
ORIGINAL ω_o = 61 %
BROWN VARVED CLAY
α = 9.4°
ϕ_u = 9.5°
q, $\frac{(\sigma_v-\sigma_h)}{2}$ — psi
p, $\frac{(\sigma_h+\sigma_v)}{2}$ — psi
0
2
4
6
8
10
12
14
16
18
20
22
24
0
10
20
30
40
50
60
70

Fig 12

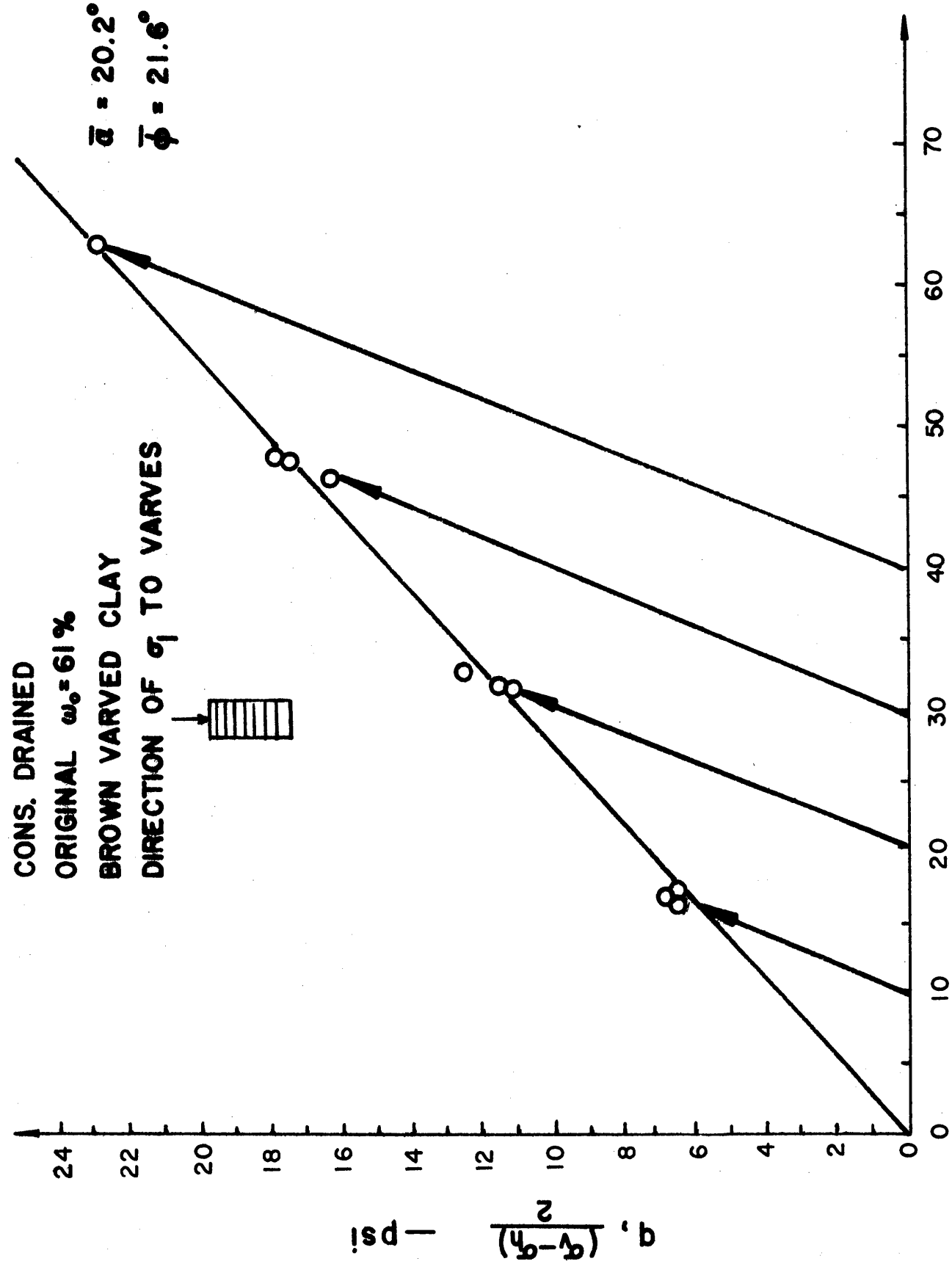
CONS. DRAINED
ORIGINAL ω_o = 61 %
BROWN VARVED CLAY
DIRECTION OF σ_1 TO VARVES
$\bar{a}$ = 20.2°
$\bar{\phi}$ = 21.6°
$q, \frac{(\sigma_1-\sigma_3)}{2}$ — psi
$\bar{p}, \frac{(\bar{\sigma}_v+\bar{\sigma}_h)}{2}$ — psi
0
2
4
6
8
10
12
14
16
18
20
22
24
0
10
20
30
40
50
60
70

FIG 13

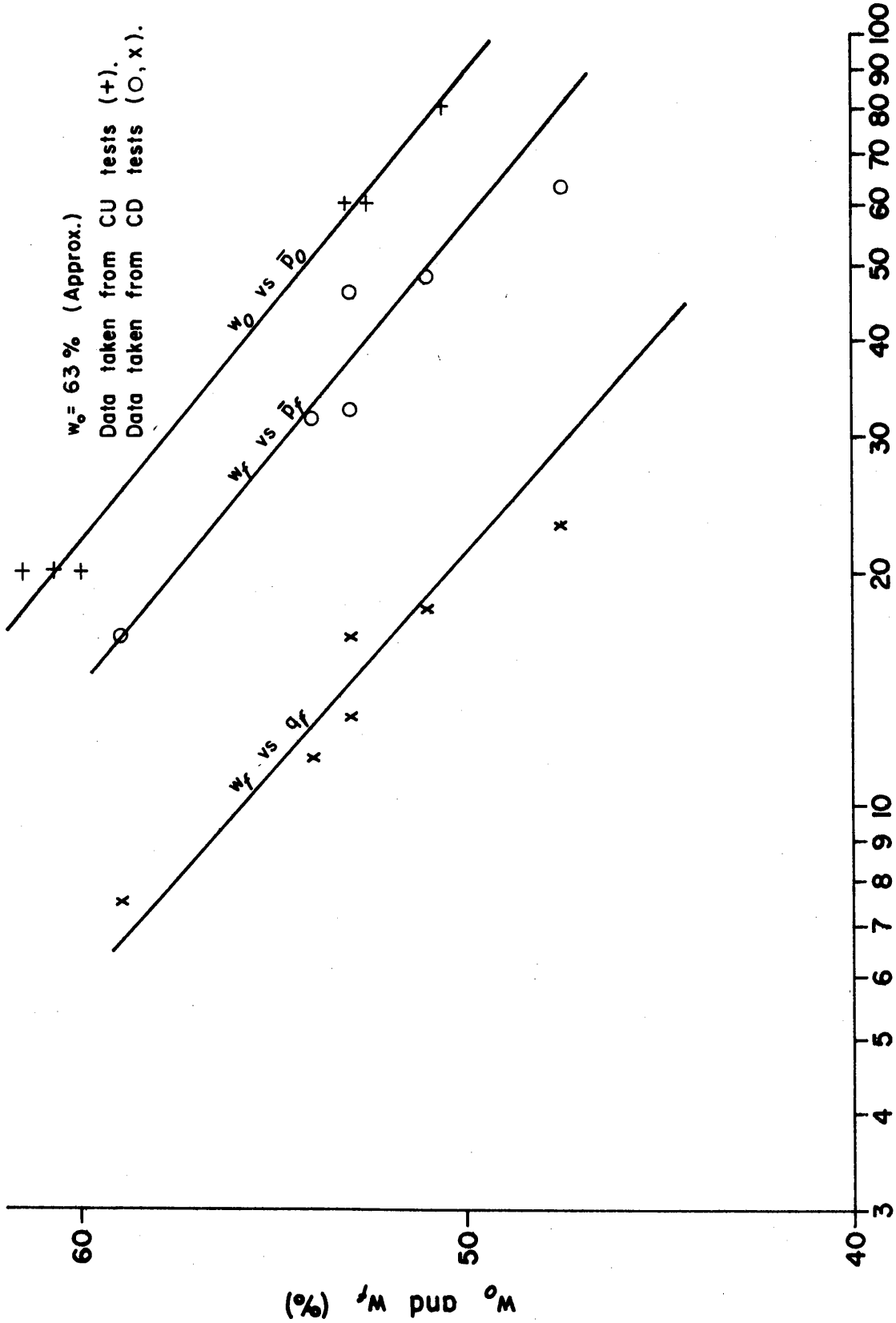
w_o= 63 % (Approx.)
Data taken from CU tests (+).
Data taken from CD tests (○, x).
w_o vs $\bar{p}_o$
w_f vs $\bar{p}_f$
w_f vs q_f
w_o and w_f (%)
60
50
40
q_f, $\bar{p}_o$, $\bar{p}_f$ (psi)
3
4
5
6
7
8
9
10
20
30
40
50
60
70
80
90
100

Fig 14

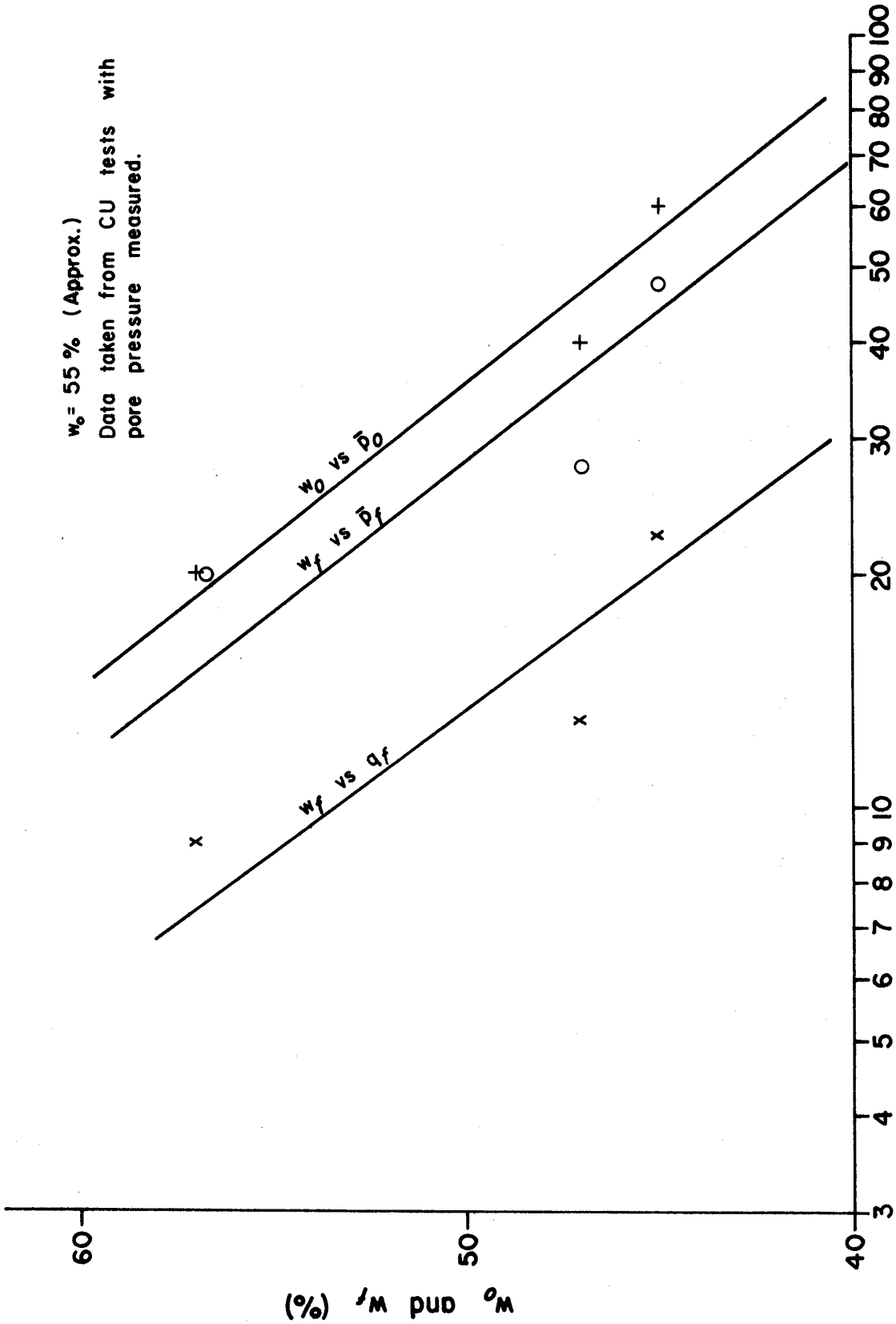
w_o and w_f (%)
60
50
40
q_f, $\bar{p}_o$, $\bar{p}_f$ (psi)
3
4
5
6
7
8
9
10
20
30
40
50
60
70
80
90
100
w_o vs $\bar{p}_o$
w_f vs $\bar{p}_f$
w_f vs q_f
w_o = 55 % (Approx.)
Data taken from CU tests with pore pressure measured.

Fig 15

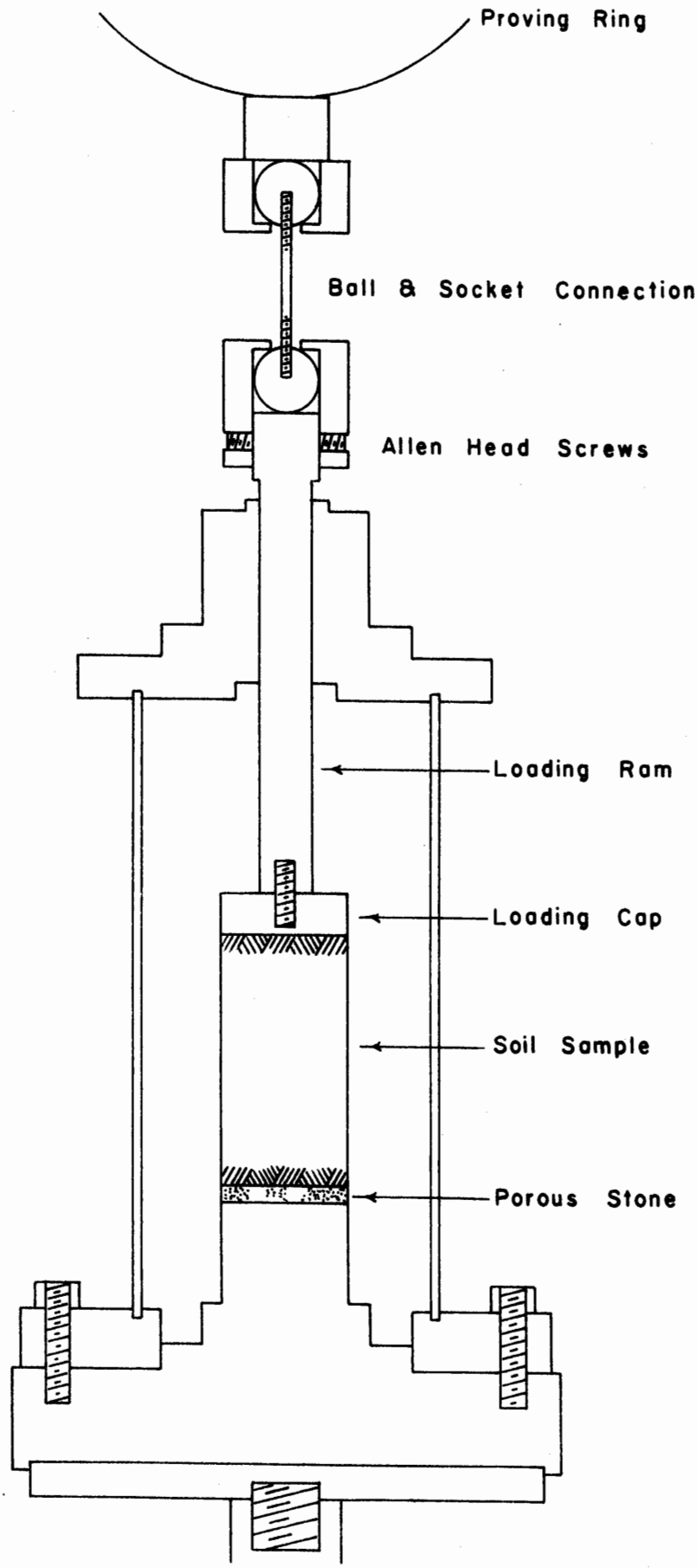

RAM ATTACHMENT FOR
TRIAXIAL EXTENSION TEST

Fig 16

SKETCHES OF SAMPLE FAILURE

45°

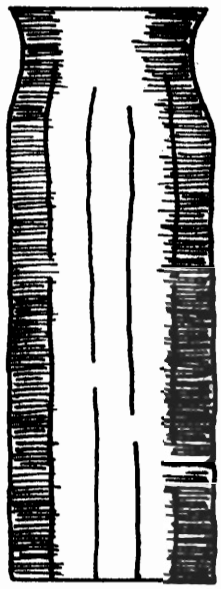

90°

0°

45°

30°

60°

Orientation of varves with respect to the major principal axis is given in degrees under each sketch.

Fig 17

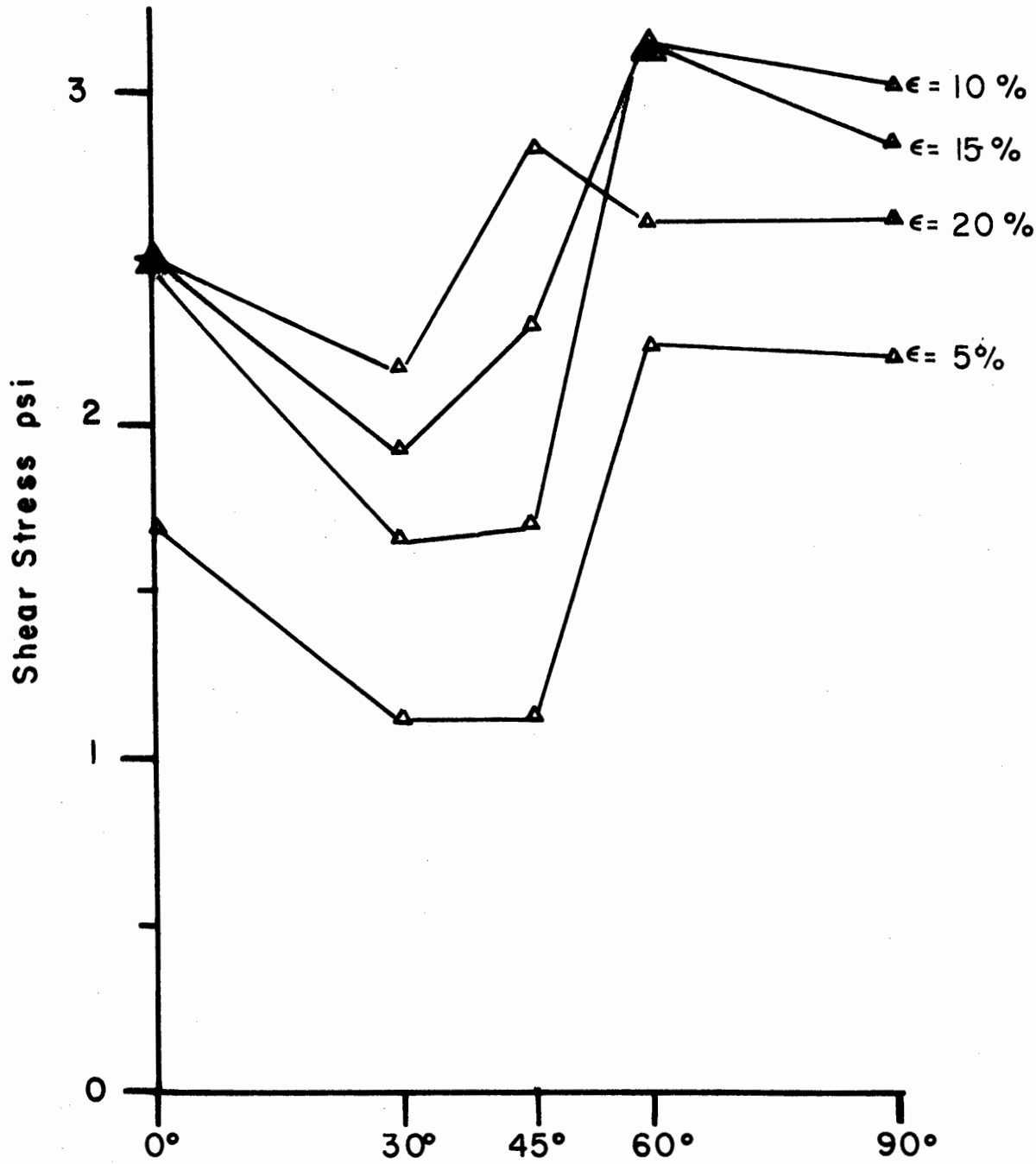

Extension Test Results

Fig 18

APPENDIX

Time to Failure Computation

Times to failure for the samples used in the consolidated-drained tests and the consolidated-undrained tests with pore pressure measurements were computed beforehand and the apparatus adjusted for the appropriate strain rate. Time to failure (t_f) for the consolidated drained test was computed from: (1)*

$$\bar{U}_f = 1 - \frac{h^2}{\eta C_v t_f} \qquad (1)$$

where: $\bar{U}_f$ = the average degree of dissipation of pore pressure desired at failure, taken as 95%;

h = 1/2 the height of sample; C_v = coefficient of consolidation in $(\text{length})^2/\text{time}$; t_f = time to failure; η = a factor depending on the drainage conditions. The units for h, C_v and t_f must be selected so that the equation becomes dimensionless. The term η is dimensionless.

The values of η are shown in Table II for the most common drainage conditions used in triaxial testing. Filter-paper drains were used around the samples for the CD tests. A value of $\eta = 32.0$ was used to find the time to failure, although the sample drained a little faster because the bottom end was in contact with a porous stone.

Table II

Drainage Conditions	η
Drainage from one end only	0.75
both ends	3.0
radial boundary only	32.0

*Numbers in parentheses indicate references at the end of the appendix.

The time to failure was computed using the coefficient of consolidation exhibited by the specimen during the consolidation phase of the test. The computed times to failure varied from 2 to 47 hours. The rate of strain was then selected from the time to failure and the anticipated strain at failure. The anticipated strain at failure was approximated from previous tests.

During many of the undrained tests pore pressure measurements were made at the base of the specimen. The pore pressure measurements were made with a Dynisco pressure tranducer connected to a Hewlett-Packard 710B Strip Chart Recorder with 17505A plug-ins. The pressure transducer sensed the pore pressure at the bottom of the sample through a connection on the base of the triaxial cell. The pressure transducer was screwed into the connection when the base plate was under water to insure that no air bubbles were trapped in the line. The transducer was calibrated by applying pressure to the triaxial chamber containing no sample but completely filled with water.

The speed of testing must be regulated when pore-pressure measurements are taken. As the shear stresses are applied the pore pressures at the ends of the specimen may be different from the pore pressure at the center of the specimen where failure will occur. To insure that the measured pore pressure represents the pore pressure on the failure plane the speed of testing has to be regulated. A time to failure must be selected that is long enough to allow the pore pressures within the specimen to equalize throughout the specimen.

The time to failure was selected from Table III (2).

In Table III η = the equalization ratio and can be defined by the equation:

$$\eta = \frac{(u'_e - u'_c)}{(u_e - u_c)} \qquad (2)$$

where: u'_e = pore pressure at the ends of the specimen at failure in force/unit area

u_e = pore pressure at the ends of the specimen under rapid loading, in same units

u'_c = pore pressure at the center of the specimen at failure, in same units

u_c = pore pressure at the center of the specimen under rapid loading in same units.

The time factor "T_f" is defined as:

$$T_f = \frac{C_v}{h^2} t_f \qquad (3)$$

where: C_v = coefficient of consolidation in $(\text{length})^2/\text{time}$

h = 1/2 the height of the specimen in the same length units used for C_v

t_f = time to failure in the same time units used in C_v

TABLE III

T_f	η	T_f	η
0	1.0	0.66	0.15
0.001	0.95	0.79	0.105
0.01	0.85	1.0	0.08
0.1	0.53	1.67	0.05
0.2	0.36	1.9	0.04
0.3	0.27	2.7	0.03
		4.0	0.02

Theoretically, the pore pressure in the center is never exactly equal to the pore pressure on the ends of the specimen. However, as a practical approach, 90 to 95% equalization is satisfactory. A percent equalization of 95 (η = 0.05)

was used in these tests. The time to failure was determined from the appropriate time factor (T_f = 1.67 in this case) using the proper C_v and h values for each specimen. The amount of strain at failure was approximated from previous tests and from these the proper rate of strain was set on the triaxial apparatus. For the UU tests, the time to failure was about 2 hours. As the consolidation pressure increased the coefficient of consolidation decreased resulting in a longer time to failure. The time to failure for some of the consolidated-undrained tests ran as long as 7 hours.

References

1. Bishop, A. W. and Henkel, D. J., "The Measurement of Soil Properties in the Triaxial Test", Edward Arnold Ltd., London, 1957. p. 125.

2. Schiffman, R. L., "Theory of Consolidation Class Notes", Rensselaer Polytechnic Inst., Troy, N. Y. 1964 (Unpublished)